Clim Dyn (2012) 38:75–86
DOI 10.1007/s00382-011-1103-4

A 40-year accumulation dataset for Adelie Land, Antarctica and its application for model validation

Cécile Agosta · Vincent Favier · Christophe Genthon · Hubert Gallée · Gerhard Krinner · Jan T. M. Lenaerts · Michiel R. van den Broeke

Received: 22 June 2010 / Accepted: 16 May 2011 / Published online: 4 June 2011

Abstract The GLACIOCLIM-SAMBA (GS) Antarctic accumulation monitoring network, which extends from the coast of Adelie Land to the Antarctic plateau, has been surveyed annually since 2004. The network includes a 156-km stake-line from the coast inland, along which accumulation shows high spatial and interannual variability with a mean value of 362 mm water equivalent a^{-1}. In this paper, this accumulation is compared with older accumulation reports from between 1971 and 1991. The mean and annual standard deviation and the km-scale spatial pattern of accumulation were seen to be very similar in the older and more recent data. The data did not reveal any significant accumulation trend over the last 40 years. The ECMWF analysis-based forecasts (ERA-40 and ERA-Interim), a stretched-grid global general circulation model (LMDZ4) and three regional circulation models (PMM5, MAR and RACMO2), all with high resolution over Antarctica (27–125 km), were tested against the GS reports. They qualitatively reproduced the meso-scale spatial pattern of the annual-mean accumulation except MAR. MAR significantly underestimated mean accumulation, while LMDZ4 and RACMO2 overestimated it. ERA-40 and the regional models that use ERA-40 as lateral boundary condition qualitatively reproduced the chronology of interannual variability but underestimated the magnitude of interannual variations. Two widely used climatologies for Antarctic accumulation agreed well with the mean GS data. The model-based climatology was also able to reproduce the observed spatial pattern. These data thus provide new stringent constraints on models and other large-scale evaluations of the Antarctic accumulation.

Keywords Mass balance · Antarctica · Accumulation · Spatial variability · Temporal variability · Model validation

C. Agosta (✉) · V. Favier
UJF-Grenoble 1 / CNRS, Laboratoire de Glaciologie et de Géophysique de l'Environnement UMR 5183, 54 rue Molière, BP 96, 38402 Saint Martin d'Hères Cedex, France
e-mail: agosta@lgge.obs.ujf-grenoble.fr

C. Genthon · H. Gallée · G. Krinner
CNRS / UJF-Grenoble 1, Laboratoire de Glaciologie et de Géophysique de l'Environnement UMR 5183, 54 rue Molière, BP 96, 38402 Saint Martin d'Hères Cedex, France

J. T. M. Lenaerts · M. R. van den Broeke
Institute for Marine and Atmospheric Research Utrecht, Utrecht University, Utrecht, The Netherlands

1 Introduction

In the context of global climate change (IPCC 2007), particular attention is being paid to the mass balance of the Antarctic ice sheet and its impact on the rise in sea level. The changes in the Surface Mass Balance (SMB) of Antarctica are considered as a second order problem because surface accumulation has not changed significantly over the last 50 years compared with the accelerated mass loss at the ice sheet boundaries (Rignot et al. 2008). However, the ice sheet interior shows a slightly increasing elevation suggesting a mass gain due to accumulation change (e.g., Helsen et al. 2008) and most coupled general circulation models predict that the SMB of the ice sheet will increase in a warmer climate (Krinner et al. 2007). It is worth noting that a 10% increase in mean Antarctic precipitation would roughly represent a global sea level decrease of about 5 mm $decade^{-1}$, which is not negligible compared to dynamic mass losses on ice sheet margins. Hence,

estimating possible sea level rise mitigation by the snowfall driven growth of the Antarctic ice sheet is of importance. However, direct SMB data from stake measurements, ice core and surface radar analysis are sparse and generally cover too short time span and too low resolution to allow us to assess whether any significant change has already occurred. In spite of the contribution of satellite remote sensing (passive micro wave) to extrapolate local measurements (Arthern et al. 2006), even assessments of the mean total SMB of Antarctica are still subject to significant uncertainties (Mayewski et al. 2009). Increasing the density of direct field measurements and monitoring over the ice sheet is thus imperative. This is particularly true in low elevation coastal areas where much of the future SMB change is expected to occur (e.g., Krinner et al. 2007; Genthon et al. 2009) but field observations and reports are comparatively rare in the lower elevation parts of Antarctica.

In coastal Adelie Land, the set out of a stake-line from Cap Prudhomme at the coast to 156 km inland was initiated in early 2004 (Fig. 1). This network is part of the GLACIOCLIM (the GLAciers, an Observatory of CLIMate)-SAMBA (SurfAce Mass Balance of Antarctica) observatory. Some reports of annual snow accumulation between 1971 and 1992 are available from IPEV (*Institut Polaire Francais Paul-Emile Victor*) archives in the vicinity of the part of the GLACIOCLIM-SAMBA (hence referred to as GS) stake-line located closest to the coast, which can be used to evaluate changes that have occurred in the last 40 years in the area. Most of these older reports are unpublished, while some of the data previously listed by Pettré et al. (1986) were re-analyzed and processed for the present study.

In this paper, GS measurements are compared to the older reports (from now on referred to as IPEV data) to assess the spatial and temporal variability of the SMB in coastal Adelie Land. The mesoscale accumulation pattern along the GS stake-line is also used to validate accumulation from meteorological or climate models or from extrapolations of field observations. After describing the climate settings in Sect. 2, we present the data and the methods in Sect. 3. In Sect. 4, we present the results of the comparison of GS and IPEV data, highlighting the fact that the accumulation pattern has changed little over the last 40 years. We also report how climitologies and model results agree with the observed variability of accumulation. Finally, we discuss the possible reasons for discrepancies and we present our conclusions in Sect. 5.

2 Climate settings

Cap Prudhomme (CP, 66.7°S, 139.9°E, 30 m above sea level) hosts a summer station at the departure point of the logistical traverse between the coast and the French-Italian Concordia station located ~1,100 km inland at Dome C on the plateau. The CP station is located 5 km from the permanent French station in Adelie Land, Dumont d'Urville, for which the mean meteorological conditions have been reported by König-Langlo et al. (1998). In pace with solar radiation influx, the temperature shows a strong seasonal cycle that has significant consequences for accumulation/ablation processes. The annual mean air temperature is −10.8°C. Precipitation is mainly solid and only a few rare cases of drizzle and rainfall have been reported (König-Langlo et al. 1998). Melting only occurs during summer months (December to February) and represents an insignificant contribution to the SMB. The coast of Adelie Land is affected year round by low-pressure systems from the North West (König-Langlo et al. 1998) that intrude into the continent and adiabatically cool as they rise along the topography. Cyclones rarely penetrate deep into the interior but certainly affect much of the area sampled by the GS stake-line. Due to blowing snow, precipitation sampling is complicated, and is usually deduced from net accumulation analysis (König-Langlo et al. 1998). One of the main climate characteristics in the area is the strong temperature inversion on slopes and relative negative buoyancy forces,

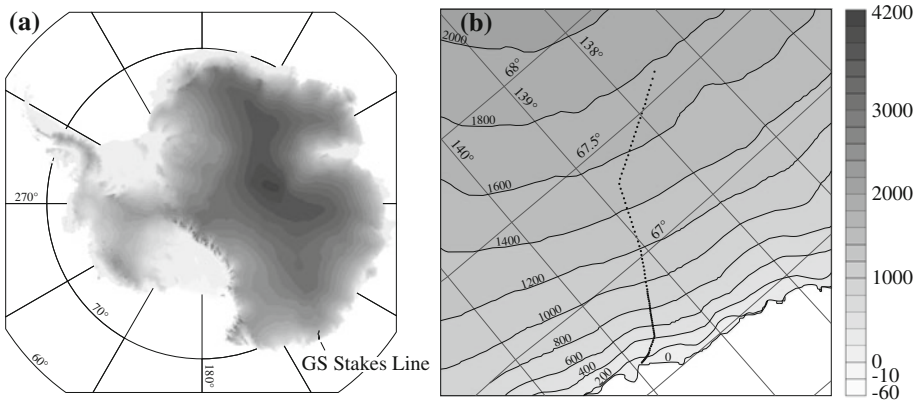

Fig. 1 Surface elevation in m from Bamber et al. (2009) and location of the GS stake-line

which are responsible for strong persistent katabatic winds (Gallée and Pettré 1998). Because of high wind velocities and steep relief along the coast, the distribution of precipitation may be affected by gravity waves or even by the Loewe effect (King and Turner 1997). Finally, along the sea front in Adelie Land, snow erosion by the katabatic winds leads to net ablation resulting in areas of blue ice (Genthon et al. 2007).

3 Data and methods

3.1 GLACIOCLIM-SAMBA and IPEV stake measurements

3.1.1 Field data

The SMB data used here are the following (Table 1):

- Annual SMB values (stake height and density measurements) from the 156-km GS stake-line (91 stakes), collected between 2004 and 2008 (5 years);
- Annual stake height measured by IPEV from 1.0 to 16.5 km from Cap Prudhomme station (22 stakes) between 1971 and 1992 (21 years).

The GLACIOCLIM observatory is a French initiative to monitor the mass balance of glaciers in different climate environments from the Tropics to the Polar Regions. Its Antarctic component covers Adelie Land and Dome C. The SMB of Antarctica is the net result of precipitation and surface ablation terms like evaporation/sublimation, melt and run-off, and blowing snow. The SMB at a particular site cannot be correctly sampled by a single stake because of small-scale spatial noise due to deposition and post-deposition processes (e.g., sastrugis) (Genthon et al. 2005). Thus, for local monitoring, stake networks are recommended (Eisen et al. 2008). However deploying and surveying many stake networks along more than 150 km every year would be a huge logistical challenge. To sample spatial scales consistent with those of climate models, a stake-line is the best trade-off. In our case, the GS accumulation stake-line along the logistical traverse to Concordia station was used. The stake-line extends 156 km in the transition zone between the coast (almost sea level) and the interior plateau (1,819 m above sea level, see Fig. 2). This is where ocean-continent contrasts and varied topography produce some of the sharpest meso-scale gradients. The GS stake-line is thus ideally designed to test models at scales close to their spatial resolution in that part of Antarctica with high mean accumulation.

Measurement protocols and accuracy are described in detail in Eisen et al. (2008). The stakes are 4 m polycarbonate poles inserted approximately 1 m into the snow surface. A stake is replaced when the emerging part is deemed too small to guarantee that it will not be completely buried by the end of the following year. The replacement stake is placed where the first stake in the series was initially located. The annual ice surface motion as measured with a navigation GPS (accurate to 10 m in this region) reaches up to 80 m per year 32 km from the coast, averaging 45 m per year along the stake-line. No stake could have moved more than 150 m before being replaced back to its initial position. A wooden stick (anchor) guarantees that the end of the pole buried in the snow remains fixed with respect to the surrounding snow layer. Thus, leaving aside the contribution of the variability of spatial accumulation to a stake moving with the surface before it is replaced, any change in the height of the pole above the snow level is due to either snow accumulation or snow densification between the surface and the anchor. Measuring the height of the pole and the snow density above the anchor makes it possible to retrieve the mean SMB between two campaigns. Surveys are made in January of each year. The snow density of the first 2.5 m or deeper at each stake is obtained from snow cores (Fig. 2).

Data mining in the IPEV archives enabled retrieval of older accumulation data. From 1971 to 1992, IPEV staff recorded the snow height of 22 navigation stakes from the

Table 1 SMB observations along the stake-line from Cap Prudhomme inland

	IPEV gap filled 1.0–16.5 km	GS 1.0–16.5 km	GS 0–52 km	GS 0–104 km	GS 0–156 km	GS gap filled 0–156 km
Number of stakes	22	20	50	71	91	91
Period	1971–1991	2004–2008	2004–2008	2005–2008	2006–2008	2004–2008
Number of years	21	5	5	4	3	5
SMB mean, mm w.e. a^{-1}	265	268	385	327	296	358
SMB weighted mean, mm w.e. a^{-1}	299	296	406	330	291	355
SMB standard deviation, mm w.e. a^{-1}	135	158	211	184	179	180

The weighted mean is computed by weighting the SMB of each stake with the distance between two adjacent stakes

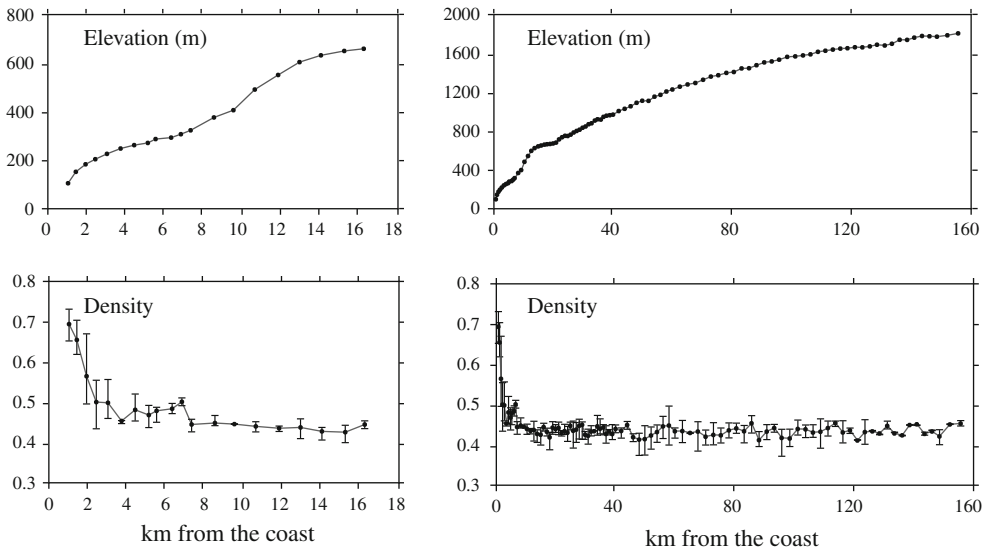

Fig. 2 Snow density and surface elevation profiles along the stake-line. Density is given at a depth of 2.5 m, with vertical bars delimiting the minimum and maximum density values observed between 2004 and 2009. Elevation is evaluated by navigation GPS

coast to 17 km inland. Although no GPS was available to accurately and regularly measure the position of the stakes, occasional sun positioning confirms that the older stake-line followed the present logistical path to Dome C and thus coincides with the part of the GS line close to the coast. Screening of the initially hand-written reports revealed some inconsistencies, e.g. exceptional increases or decreases in accumulation in a given year, probably due to an unreported stake replacement. Part of the dataset was consequently not used, and some of the remaining reports may be less reliable than others. In addition, a new stake was inserted only when the previous stake had been completely buried and could not be retrieved. Otherwise, a new length of pole was simply attached to the previous one. However, the ice motion reaches a maximum of 40 m a^{-1} in this area, so the distance to the initial point is estimated to have a maximum uncertainty of 500 m.

The IPEV stakes were not anchored to a given snow layer, and no density measurements were made. Pettré et al. (1986) used some of the IPEV observations and converted them into water-equivalent using an empirical density profile. However, density measurements along the GS line have since revealed that the empirical density profile used by Pettré et al. (1986) is not appropriate so close to the coast where melting and ice lenses can occur. However, the GS density measurements in the 2004–2008 period show limited interannual variability (Fig. 2, the mean of the relative standard deviation was less than 5%) despite significant variability in accumulation. We thus chose to use the mean GS densities to convert the IPEV snow accumulation reports to water-equivalent accumulation.

We also display the most reliable accumulation data from shallow ice-cores sampled between 1976 and 1983 near the current GS stake-line, obtained by dating reference horizons of anthropogenic radionuclide. This measurement technique, which is deemed to be very reliable (Magand et al. 2007), resulted in 10-year to 28-year mean SMB values covering the 1955–1983 period. The major uncertainties associated with these measurements concern the accuracy of their location and the bias caused by the ice flow, since the surface ice speed is high and accumulation is highly variable at the kilometer scale in the region.

3.1.2 Missing data and gap filling

Different kinds of data were missing in the IPEV and GS series. It took three field seasons to complete the GS stake line. Forty-one stakes were first set out up to 52 km from the coast, then 20 additional stakes up to 105 km the following season. The line was completed with 91 stakes up to 156 km in the third season in 2006. Gap filling was necessary to obtain a consistent dataset for the 5 years of measurement along the full 156 km-line. However, no bulk gap filling was necessary for missing years in the GS dataset when comparing it with the IPEV data in the 17 km closest to the coast. Twenty-four percent of IPEV data were missing, but the gaps were randomly spread out over the 22 stakes and 21 years concerned.

Despite these differences, we used the same method to fill gaps in the two datasets. This method is based on the EOF analysis of the SMB spatial variability. EOF analysis is carried out using the covariance matrix of the data centered to zero mean. It yields the centered spatial modes (EOFs) of the SMB and the associated time series. The EOFs are sorted according to the percent of total variability they account for, the first EOF (EOF1) explaining the greatest portion of total variance. To extract the main spatial pattern, we only needed retain the most significant EOFs. To this end, we created random datasets of the same size as the original data. Random values were generated for

each year from normal distributions with means and standard deviations equal to those of the original data. We selected EOFs that were significantly different from noise as those for which the associated eigenvalues were higher than the ones from randomly-generated datasets.

Along the first 50 GS stakes from the coast to 52 km inland, the first EOF was very similar whether calculated for 2004–2008 or 2006–2008 (Fig. 3). Thus it may reasonably be assumed that beyond 52 km, EOF1 for 2006–2008 is a good estimator of the mean spatial variability over the 2004–2008 period. EOF analysis was performed by skipping missing data in the covariance matrix computation, so EOF1s of 2004–2008 and 2004–2006 were almost identical by construction beyond km 52. EOF1 alone explained 72% of the total variance for the 2004–2008 dataset and was thus used to represent the main spatial pattern of the GS line. Considering the IPEV dataset, EOF1 explained 50% of the total variance, but EOF2 and EOF3 were also significantly different from noise. Thus the first three EOFs were used to represent the main spatial pattern and together explained 74% of the total variance.

For both the IPEV and GS data, the linear regressions between the reconstructed time series associated with the selected EOFs and the time series of the original datasets were highly significant ($p < 0.01$), except for one particular year in the IPEV data for which p was lower than 0.02. Thus we felt confident using EOF regressions to estimate missing data in the observation datasets.

3.2 Antarctic SMB climatologies

We compared GS data to Arthern et al. (2006) and van de Berg et al. (2006) SMB climatologies, which are currently assumed to be the most defendable estimates of broad-scale patterns of SMB across Antarctica (Mayewski et al. 2009). To compare the computed SMB with stake values, we extracted the grid boxes covering at least six stakes in the GS stake-line: six grid boxes from the Arthern et al. (2006) climatology and four grid-boxes from the van de Berg et al. (2006) climatology.

The Arthern et al. (2006) remote-sensing based climatology was obtained by continuous-part universal kriging (Kitanidis 1997) of SMB field measurements over the 1950–1990 period (Vaughan and Russell 1997) with a background model based on passive microwaves data. The climatology is given at 25 km resolution, but the authors estimate the effective resolution of the map to be ~100 km, so data variability at a smaller scale should be considered with caution. Moreover the average accumulation rate over the major drainage sectors of Antarctica was estimated with a precision of 10% or better, but accumulation rates are expected to vary significantly from the gridded values at spatial scales smaller than 10^4 km^2.

The van de Berg et al. (2006) climatology is based on the Regional Atmospheric Climate Model v.2 (RACMO2) calibrated with SMB field observations. RACMO2 was run at a 55-km resolution using the version described in Sect. 3.3 without snowdrift. The lateral boundary conditions were provided by ERA-40 and operational analyses from the European Centre for Medium-range Weather Forecasts (ECMWF) for the period 1980–2004. The observation dataset is a revised version of that compiled by Vaughan and Russell (1997) plus 236 new observations.

3.3 High resolution models

Modeling was performed with different types of models with distinct resolutions, all finer than 120 km:

- The ERA-40 and ERA-Interim global atmospheric reanalyses from the ECMWF. ERA-40 fully covers the 1958–2001 period (Uppala et al. 2005), and is run on a reduced Gaussian grid with T159 spectral truncation that has a nominal resolution of 125 km. ERA-Interim is the most recent ECMWF reanalysis (Simmons et al. 2006), and covers the period 1989 to the present. The main advances of ERA-Interim over ERA-40 are a finer spectral truncation (T255, nominal resolution of 80 km), improved model physics and a more efficient data assimilation system (4D-Var instead of 3D-Var).
- An atmospheric global circulation model, LMDZ4 (Hourdin et al. 2006), which includes several improvements for the simulation of polar climates as suggested by Krinner et al. (1997). It is the atmospheric component of the IPSL-CM4 climate system model (Marti

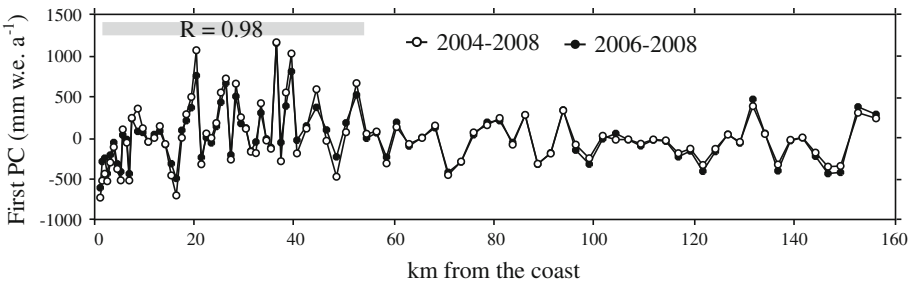

Fig. 3 EOF1 of the GS SMB measurements for 3 years of data (2006–2008, *full black circles*) and 5 years of data (2004–2008, *empty circles*). The correlation coefficient R is computed between values of these two components for the first 50 stakes up to 52 km

et al. 2006) that participated in the World Climate Research Programme's Coupled Model Inter-comparison Project phase 3 (CMIP3) exercise. Here, we use a 20-year simulation run (1981–2000) with prescribed sea surface boundary conditions (sea ice concentration and sea surface temperature) taken from CMIP3 simulations carried out with the IPSL-CM4 coupled model. Although global, LMDZ4 reaches 60-km resolution when the grid is stretched out over Antarctica. Since LMDZ4 is only forced by sea surface conditions, it is not able to display the actual chronology of interannual SMB variations.

– Three regional circulation models (RCM), (1) PMM5 and (2) MAR laterally forced by ERA-40 and (3) RACMO2 laterally forced by ERA-Interim. Models and simulations are described hereafter.

(1) The first RCM, PMM5, is fully described in Grell et al. (1994). Bromwich et al. (2001) and Cassano et al. (2001) give a detailed description of the major changes to MM5 to optimize the model for use over ice sheets like Polar MM5 (PMM5). The simulation used is detailed in Monaghan et al. (2006b) and is available on the Antarctic Hindcast Project website. The model is run over the 1981–2000 period with a 60-km resolution on a regular polar stereographic grid.

(2) The second RCM, MAR (*Modèle Atmosphérique Régional*), presents the atmospheric scheme described in Gallée and Schayes (1994) coupled to a physically based model of the snow pack (Gallée and Duynkerke 1997). A parameterization of snowdrift was also developed and tested in Antarctic conditions (Gallée et al. 2001). The simulation is run at 40 km resolution on a polar stereographic grid for the 1981–2000 period.

(3) Finally, the third RCM, the Regional Atmospheric Climate MOdel v.2 (RACMO2) is based on the High Resolution Limited Area Model (HIRLAM) with physical processes adopted from the global model of the ECMWF. Its adaptation for polar ice sheets is described in Ettema et al. (2009). Recently, RACMO2 was run at 27 km resolution over Antarctica with the snowdrift routine described in Lenaerts et al. (2010). The lateral boundary conditions are provided by ERA-Interim and the model is run over the 1989–2008 period.

GS stake values were compared to data from the corresponding model grid boxes. Grid-box selection was the same as that described in Sect. 3.2. Thus two grid boxes were retained for ERA-40, three for ERA-Interim and LMDZ4, five for PMM5 and MAR, and six for RACMO2. The models used in this study simulate precipitation and surface sublimation. The SMB is computed by subtracting the latter component from the former. Except for PMM5, the models also simulate melting and run-off, but we did not consider this term in the computation of the SMB because run-off is negligible in Adelie Land. Indeed, stratigraphic analysis of snow cores showed that ice layers caused by water percolation and refreezing seldom occur further than the first 5 km from the coast and not at all beyond 20 km. MAR and RACMO2 models consider snow erosion, snow transport by the wind and snowdrift sublimation. The contribution of blowing snow to either export to the ocean or enhanced evaporation of airborne particles is currently unknown except very close to the coast (Genthon et al. 2007) although this process may be important, particularly in coastal regions (e.g., Gallée et al. 2001; Frezzotti et al. 2004) and should be the object of forthcoming observations.

4 Results

4.1 Spatial and temporal significance of the observations

The comparison between the GS reports and IPEV measurements at each stake between 1.0 and 16.5 km from the coast is presented in Fig. 4. Spatial variability did not change significantly between 1971–1991 and 2004–2008, the minimum and maximum values over the 5-year GS data being within the 10 and 90% percentiles of the 21-year IPEV dataset. We did not calculate the percentiles of the GS data for each stake because the number of available annual reports was too small for this to be significant. On the other hand, the IPEV data are less reliable than the GS data, so percentiles allow the filtering out of extreme values. Between 1.0 and 16.5 km, the mean GS value was only 5% lower than the mean value computed from the IPEV reports. However, the data from the two stakes located at 9 and 10 km presented significantly distinct behavior, with a strong peak followed by a minimum for the IPEV SMB pattern, not shown in the mean GS record. Yet, this pattern was found in 2004, the year with the highest observed accumulation in the GS dataset. It occurred in a slope-changing area and likely derives from erosion–deposition processes close to the change in slope (Fig. 2). The temporal variability of the SMB was also of the same magnitude during the two periods (Fig. 5a). Standard deviation of the annual mean (spatially averaged) SMB was 135 mm water equivalent (w.e.) a^{-1} (156 mm w.e. a^{-1}) for the 1971–1991 period (for the 2004–2008 period, respectively) (Table 1). The relative standard

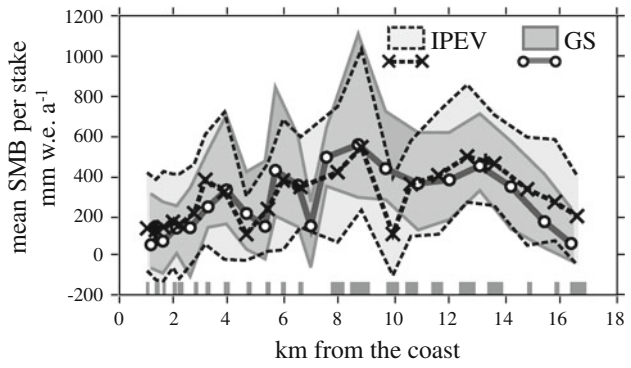

Fig. 4 Gap-filled SMB between 1.0 km and 16.5 km from the coast along the traverse between Cap Prudhomme and Dome C. The *solid black lines* and the *dark gray band* are GS SMB mean and minimum–maximum interval at each of the 20 stakes between 2004 and 2008. The *dashed black lines* and the *light gray band* are IPEV SMB mean and the 80% interval of SMB values at each of the 22 stakes between 1971 and 1991. *Gray bars* on the x-axis represent the uncertainty associated with the location of the IPEV stakes

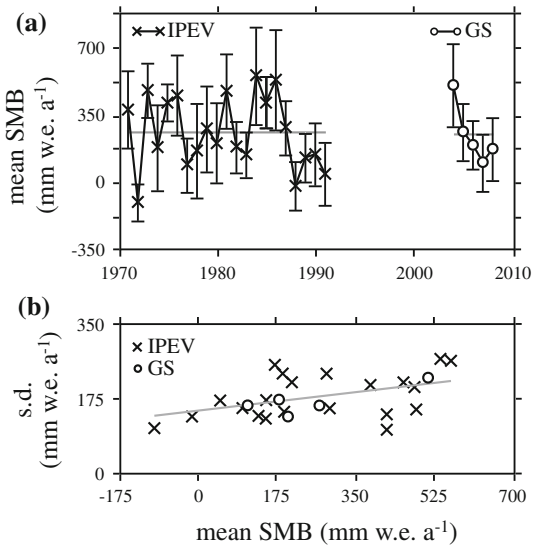

Fig. 5 Comparison between SMB computed from IPEV (*crosses*) and GS (*circles*) reports for the stakes located between 1.0 km and 16.5 km from Cap Prudhomme station. **a** The *black line* is the mean SMB, and *vertical bars* represent the two standard deviation intervals. **b** Comparison between annual mean SMB and interannual standard deviation for each stake. The *gray line* shows the linear regression for the 22 IPEV stakes

deviation over the 16 km was also similar during the two periods (Fig. 5b).

The temporal and spatial variability of the SMB in the 2004–2008 and 1971–1991 periods was remarkably similar. The 2004–2008 GS mean SMB is also in good agreement with accumulation measurements from shallow ice-cores (Fig. 6). Thus, the 5-year GS SMB data is representative of the mean SMB over longer time scales. A mesoscale pattern was observed, in which the SMB

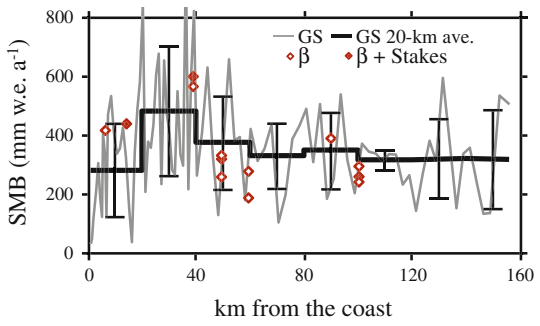

Fig. 6 Mean GS SMB for the 2004–2008 period (*thin gray line*) and 20-km mean SMB (*thick black line*). The *vertical bars* represent the 2 standard deviations of the temporally-averaged SMB values for each 20 km. The *red diamonds* are SMB measurements deduced from β-radioactive reference horizons in shallow ice cores with/without (respectively *full*/*empty diamonds*) additional stake measurements

increased from the coast up to 20–40 km and then slowly decreased towards the plateau (Fig. 6). We assumed that the regional pattern of SMB was correctly displayed by the GS stake-line and could thus be used to assess models in the study area.

4.2 Climatologies and high resolution modeling

Due to spatial resolution limitations, current climate models cannot capture the km-scale variability that is exhibited in the GS data. Understanding the processes responsible for this variability, likely related to the redistribution of snowfall and snow deposited by wind, is beyond the scope of the present study. On the other hand, it is essential that, unlike scattered stake networks, our continuous stake-line can statistically sample this variability so that it can be averaged out within the scale of a model grid box. Another key parameter for the comparison with climate models to be meaningful is the good topographic representation of the stake-line in the models. Indeed, topography is a major forcing of accumulation over Adelie Land because most of the precipitation comes from warm, moist air that arises over the land slopes. ERA-40 and ERA-Interim are the only models for which the representation of the topography differed significantly from the stake-line, due to their coarse resolution, which led to a bad distribution of the stakes over the grid boxes (Fig. 7).

On average over the study area, the mean SMB from Arthern et al. (2006) and van de Berg et al. (2006) climatologies agrees with our data (Fig. 8). This is not unexpected because both are constrained by SMB measurement of the Adelie Land area, including the β-measurements displayed in Fig. 6. However, the mesoscale variations were not reproduced by the Arthern et al. (2006) climatology whereas they were well captured by the van de Berg et al. (2006) one. Regarding climate models, MAR

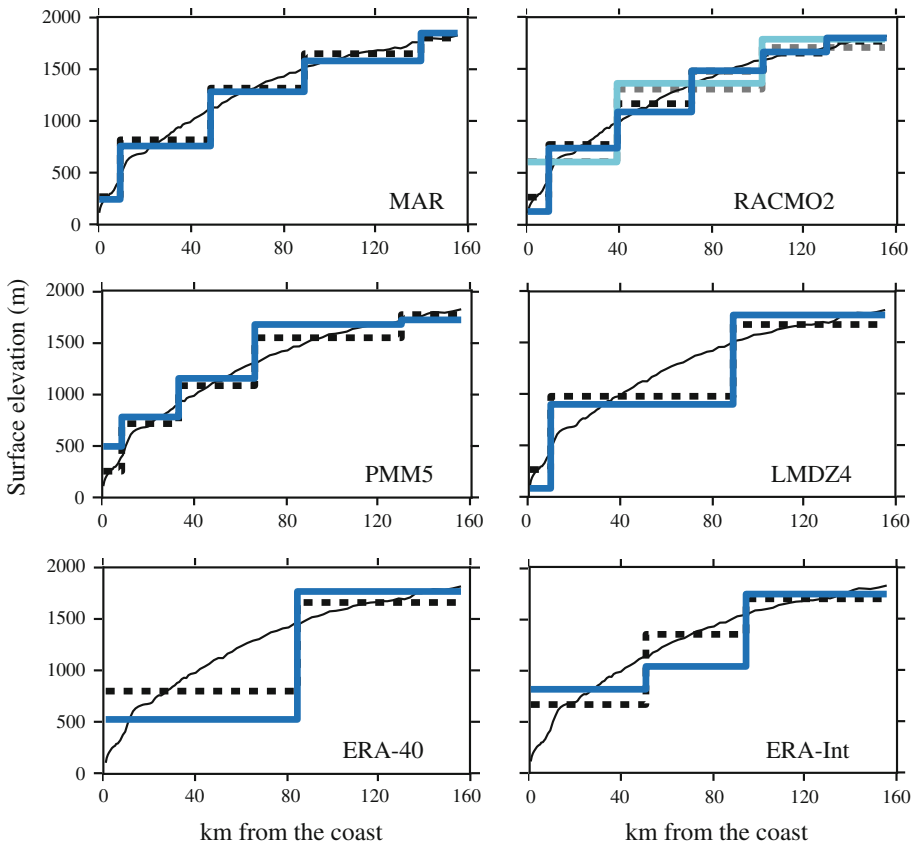

Fig. 7 Each sub-figure shows the surface elevation of the model grid boxes covering the GS stakes (*blue line*), the elevation of the GS stakes (*solid black line*) and the elevation of the GS stakes averaged over the model grid boxes (*dashed black line*). For RACMO2, the model surface elevation averaged over four grid boxes (*light blue line*) and the average elevation of the GS stakes averaged over two grid boxes (*dashed gray line*) are also given

failed to capture the mesoscale SMB increase up to 20–40 km from the coast, then the decrease towards the plateau observed along the stake-line. The other models did at least qualitatively reproduce this pattern (Fig. 8). Considering the SMB mean values, ERA-Interim and PMM5 did quite a good job, whereas MAR underestimated, and LMDZ4 and RACMO2 overestimated, the SMB in this coastal area. ERA-40 also overestimated the SMB close to the coast but this may be due to its topographical mismatch. The two models that calculate snowdrift (MAR and RACMO2), estimated that the erosion–deposition of the snow and the snowdrift sublimation have a negative contribution to the SMB in this region, with a minor impact on the SMB spatial pattern (Fig. 8).

Figure 9 shows the results of the comparison between the observed and modeled spatially-averaged SMB for the periods available. The magnitude of the modeled interannual variability was lower than that of observed variability, except for LMDZ4 and RACMO2. The fact that with MAR and PMM5, interannual variability is similar to that of the ECMWF analysis is consistent with the fact they both use ERA-40 as lateral boundary conditions. Due to observational constraints, the ERA-40 reanalysis and regional circulation models using ERA-40 as lateral boundary condition are expected to depict the chronological variability of the SMB and there was good agreement between the observed and modeled SMB time series during the 1981–1991 period within the first 20 km from the coast. Indeed, the correlations between modeled and observed time series between 1981 and 1991 are significant ($p < 0.05$), with a correlation coefficient of 0.63 for ERA-40, 0.61 for MAR and 0.70 for PMM5. This shows that in spite of the absence of the full amplitude of interannual variability, much of the large-scale circulation was correctly modeled by ERA-40 and the regional models forced by ERA-40 reanalysis.

5 Discussion and conclusion

A comparison between the (older) IPEV and (recent) GS reports points to several important characteristics and peculiarities of the SMB variations in Adelie Land. The high spatial variability of the SMB at very small time and space scales is a common feature in Antarctica (e.g., Eisen et al. 2008; Genthon et al. 2005). Our results show that in the study area, the spatial variability of the SMB was stationary at the ~1-km scale during the last 40 years, and at the 20-km scale during the last 5 years. This suggests that there are major topographic constraints on erosion/deposition processes in the area, corroborating similar results reported by Pettré et al. (1986). The maximum SMB

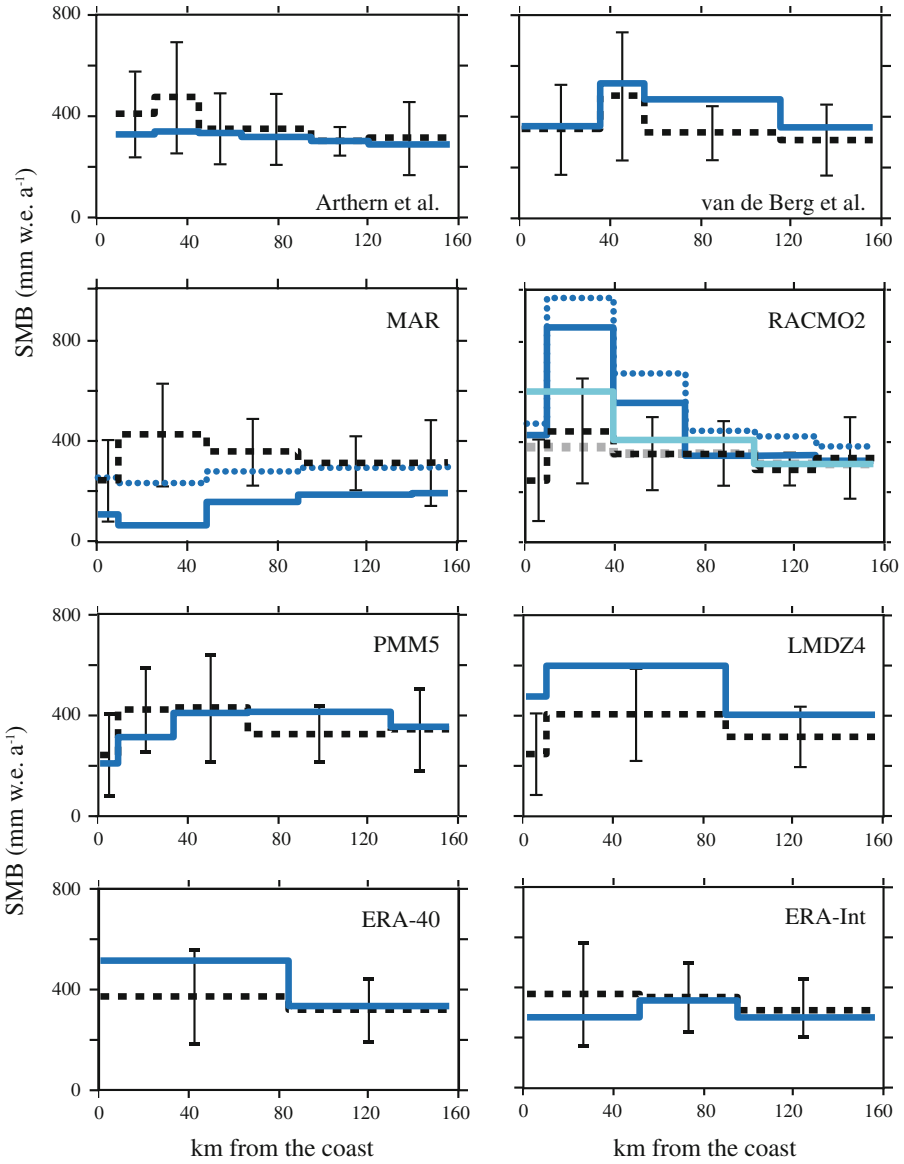

Fig. 8 Comparison between modeled and measured SMB spatial patterns. Each sub-figure shows: (1) The temporally-averaged SMB (*solid blue line*) from MAR, PMM5, LMDZ4 and ERA-40 (1981–2000 period), from RACMO2 and ERA-Interim (1989–2008 period) and from Arthern et al. (2006) and van de Berg et al. (2006) climatologies. *Dotted blue lines* represent MAR and RACMO2 SMB without snow erosion–deposition and snowdrift sublimation; (2) The GS stakes SMB averaged on each model grid box for the 2004–2008 period (*dashed black line*), with *vertical bars* representing the two standard deviations of temporally-averaged GS SMB. For RACMO2 the SMB averaged over four grid boxes (*light blue line*) and the GS stakes SMB averaged over two grid boxes (*dashed gray line*) are also shown

located around 30 km from the coast reflects the strong impact of topography on precipitation, evaporation and blowing snow, and hence on SMB distribution in the area. This common phenomenon in coastal regions (e.g., King and Turner 1997; Richardson-Näslund 2004) is hard to reproduce in models because atmospheric variables are sensitive to small-scale variations in topography close to the sea front. In addition to improved physics, higher-resolution modeling (5–10 km) would be necessary to adequately capture such effects, but limitations in computing resources prevent such resolutions at the scale of Antarctica.

Comparing the IPEV and GS data indicates that there has been little change in the mean SMB since 1970. The slight difference (around 5%) between IPEV and GS is statistically insignificant. ERA-40 and the regional circulation models forced by ERA-40 suggest a slight decrease in the late 1990s, but the ERA-40 reanalysis program stopped in August 2002. Forward trends can be studied by extending the ERA-40 data with the ECMWF operational analysis. However, there are marked differences in the meteorological and assimilation models used to produce ERA-40 and the operational analysis, in spatial resolution in particular, which make any variability and trend analysis doubtful. Yet Monaghan et al. (2006a) suggest that the decreasing trend of precipitation observed in ERA-40 after 1995 was more general at the scale of Adelie Land (see their Fig. 2) even if no significant change in snowfall has occurred since the 1950s (Monaghan et al. 2006a).

Unfortunately, the recent availability of the new ECMWF ERA-Interim reanalysis does not help in reliably

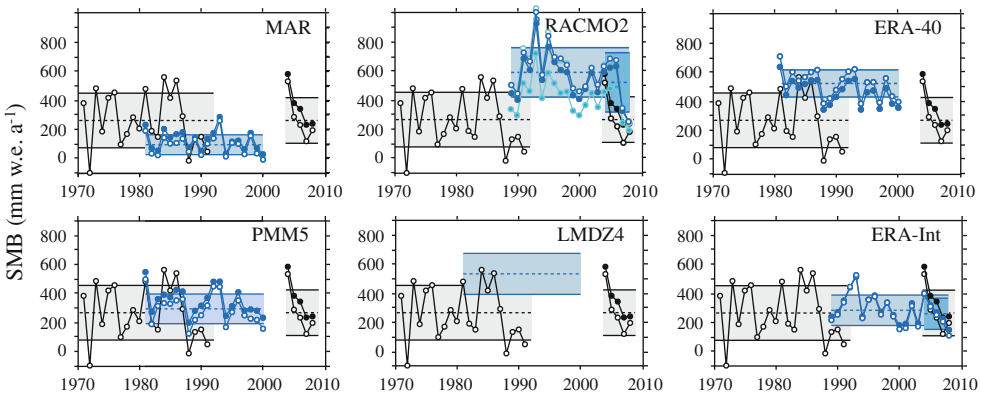

Fig. 9 Comparison between modeled and measured inter-annual variability of the SMB. *Empty circles* show the spatial mean over the location of the IPEV stakes (1.0–16.5 km from the coast) and *full circles* show the spatial mean over the 156 km GS stake-line. The *length of the boxes* shows the period of computation/measurement, the *middle dashed line* of each box shows the mean SMB over this period and the *width of the boxes* represents the two standard deviation intervals of the annual spatial mean over the location of the IPEV stakes. Each sub-figure shows the modeled (*blue lines* and *boxes*) spatially-averaged SMB and the observed (*black lines* and *gray boxes*) spatially-averaged SMB from IPEV (1971–1991) and GS (2004–2008). For RACMO2, *light blue lines* show the spatially-averaged SMB averaged over four grid boxes

evaluating recent trends since it only covers the period from 1989 to the present. Because of significant differences in the way ERA-Interim is produced (a more advanced assimilation scheme, higher spectral truncation), ERA-Interim is no more appropriate than operational analysis to tentatively complement ERA-40 over longer time scales. We do show (Fig. 10) that ERA-40 and ERA-Interim significantly differed in Adelie Land over their common period, 1989–2000. In the same period, the two reanalyses agreed well in terms of interannual variability but ERA-Interim tended to produce lower SMB values (Fig. 10a). On the other hand, ERA-Interim fully covers the time span of the GS observations, which is not the case for ERA-40. ERA-Interim also reproduced the decreasing trend in the GS record. Interestingly, precipitation was shown to be very similar in the two reanalyses over the common period (Fig. 10b). Much of the difference in SMB is due to ERA-Interim simulating much larger sublimation.

ERA-40 reproduced the interannual chronology of SMB variability in the area. This is an important result because several studies (e.g., Monaghan et al. 2006a; Helsen et al. 2008) used ERA-40 or ERA-40 driven models to extrapolate shallow core estimations of long-term SMB changes at the full scale of the Antarctic ice sheet. In spite of a number of discrepancies, the fact that the models agreed reasonably in various ways with our observations is rather encouraging. One main problem involved in validating the models for the prediction of changes in Antarctic SMB and of their impact on sea level is that they tended to underestimate the observed magnitude of natural interannual variability, except for RACMO2, driven by ERA-Interim, and for LMDZ4, the atmospheric component of one of the IPCC-AR4 models, which is free from any meteorological observational constraint. This is surprising because models that use observed sea ice, such as ERA, would be expected to do better in depicting the absolute amount of precipitation than AR4 models, since precipitation and evaporation rates depend on the extent of sea ice. A more detailed consideration of interactions between ocean, sea ice and atmosphere might provide a better representation of the

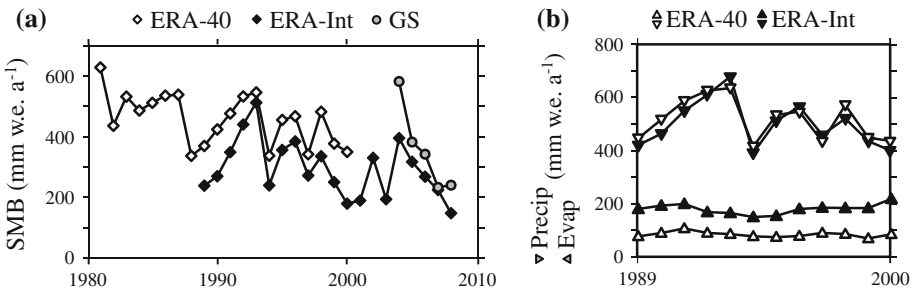

Fig. 10 Comparison of annual mean SMB from ERA-40, ERA-Interim and GS over the 156 km GS stake line. **a** *Empty diamonds* are ERA-40, *full diamonds* are ERA-Interim and *gray circles* are GS data. **b** Detailed components of the SMB for ERA-40 (*empty triangles*) and ERA-interim (*full triangles*). *Downward triangles* represent precipitation and upward ones sublimation

strength and frequency of storms and thus of SMB interannual variability.

On the other hand, our data proved to be a stringent test for MAR, which was specifically developed for polar climates. Several studies (e.g. Gallée and Pettré 1998) showed previously that MAR very successfully reproduced many aspects of polar meteorology and climate. Yet the agreement with our new SMB observations in Adelie Land is rather disappointing, since MAR underestimated the SMB even without taking blowing snow into account (Fig. 8), which means that precipitation was underestimated. This raises questions concerning as yet insufficiently explored aspects of the model, here probably partially related to the handling of moisture fluxes at the lateral boundary conditions.

Even with contradictory representations of the SMB in the Adelie Land area, MAR and RACMO2 made very similar estimations of snowdrift along the GS stake-line (Fig. 8), with a mean negative contribution to the SMB of 127 mm w.e. a^{-1} by MAR and of 91 mm w.e. a^{-1} by RACMO2. For both models the contribution was mainly dominated by snowdrift sublimation. Thus, the overestimation of the SMB by RACMO2 was not due to the new blowing snow parameterization. We observed that fluctuations of the RACMO2 SMB of about ± 200 mm w.e. a^{-1} between consecutive grid boxes were common in the area up to 100 km from the coast. These strong gradients were caused by small-scale topographic features, which were partly resolved by RACMO2 but not by the other models with lower horizontal resolution. We can consider a horizontal resolution equivalent to those of the other models by averaging the SMB over 4 RACMO2 grid boxes (horizontal resolution of ~ 54 km). We then obtain a more moderate overestimation of the SMB over the first 100 km from the coast (32% instead of 53%, see Figs. 8, 9), while the stake-line topography is still well represented by the grid-box average (Fig. 7). If we assume that MAR and RACMO2 snowdrift computations are realistic estimations of the contribution of blowing snow to the SMB, then LMDZ4 SMB would come closer to the observation by taking snowdrift into account, whereas PMM5 SMB may be underestimated.

The mean decade SMB climatologies of Antarctica present correct mean values in the Adelie Land area. However, the climatology of van de Berg et al. (2006) shows more details in the coastal areas than that of Arthern et al. (2006), as one would expect considering the restrictions related to the use of microwaves data in areas where slopes are strong and melting events can occur (Magand et al. 2008) in addition to the limited resolution (Sect. 3.2). The model-driven climatology is consequently more relevant than the remote-sensing based climatology in coastal areas, but the use of the former for model validation requires more care to avoid circular reasoning than for satellite data (Eisen et al. 2008).

To conclude, the results presented here show that after six successful years in operation, the GLACIOCLIM-SAMBA SMB observatory does provide valuable data to evaluate interannual and decadal SMB changes and the sensitivity of a range of climate models. Indeed, GS field observations adequately sample small-scale spatial variability to be properly averaged out, with a large spatial extent to fit the scales resolved by the models. In addition, GS data have annual resolution over a multi-year time span, which implies annual field activity over a significant number of years and thus substantial logistical supports. The GS observatory was designed to evaluate and validate climate models at the mesoscale and at interannual time scales at the periphery of the ice sheet where present accumulation and predicted change are largest. Such data are of a major importance because the reliability of a climate model that was unable to correctly reproduce such variability would be questionable with respect to its ability to predict the impact of climate warming on the Antarctic SMB and consequently on sea level. Other available data are generally not appropriate because either time or space scales do not meet the requirements for comparison with models. We distribute the GS data (http://www-lgge.ujf-grenoble.fr/ServiceObs/SiteWebAntarc/background.html) and will continue to do as future annual campaigns provide more, so that an optimal use can be made of this data by the larger community.

Acknowledgments The GLACIOCLIM-SAMBA observatory is supported by IPEV (*Institut Polaire Paul-Emile Victor*) and INSU (*Institut National des Sciences de l'Univers*). IPEV also provided archives of older SMB measurements. Data mining, processing and analysis were done as part of Europe's FP4 Ice2sea and the French INSU/LEFE CHARMANT programs. We acknowledge the ice2sea project, funded by the European Commission's 7th Framework Programme through grant number 226375, ice2sea manuscript number 023. IDRIS (*Institut du Développement et des Ressources en Informatique Scientifique*) provided computing time for the MAR and LMDZ4 models. We thank the Antartic Hindcast Project (http://www.polarmet.osu.edu/PolarMet/ant_hindcast.html) for sharing Polar MM5 simulation results. Many people at IPEV and at LGGE have contributed to make the GLACIOCLIM-SAMBA system deployment and annual campaigns successful. We thank the three anonymous reviewers for their constructive comments.

References

Arthern RJ, Winebrenner DP, Vaughan DG (2006) Antarctic snow accumulation mapped using polarization of 4.3-cm wavelength microwave emission. J Geophys Res 111:D06107. doi: 10.1029/2004JD005667

Bamber JL, Gomez-Dans JL, Griggs JA (2009) Antarctic 1 km digital elevation model (DEM) from combined ERS-1 radar and ICESat laser satellite altimetry. National Snow and Ice Data Center, Boulder

Bromwich DH, Cassano JJ, Klein T, Heinemann G, Hines KM, Steffen K, Box JE (2001) Mesoscale modeling of katabatic winds over Greenland with the polar MM5. Mon Weather Rev 129(9):2290–2309

Cassano JJ, Parish TR, King JC (2001) Evaluation of turbulent surface flux parameterizations for the stable surface layer over Halley, Antarctica. Mon Weather Rev 129(1):26–46

Eisen O, Frezzotti M, Genthon C et al (2008) Ground-based measurements of spatial and temporal variability of snow accumulation in east Antarctica. Rev Geophys 46(1):RG2001. doi:10.1029/2006RG000218

Ettema J, van den Broeke MR, van Meijgaard E, van de Berg WJ, Bamber JL, Box JE, Bales RC (2009) Higher surface mass balance of the Greenland ice sheet revealed by high-resolution climate modeling. Geophys Res Lett 36:L12501. doi:10.1029/2009GL038110

Frezzotti M, Pourchet M, Flora O, Gandolfi S (2004) New estimations of precipitation and surface sublimation in East Antarctica from snow accumulation measurements. Clim Dyn 23:803–813. doi:10.1007/s00382-004-0462-5

Gallée H, Duynkerke PG (1997) Air-snow interactions and the surface energy and mass balance over the melting zone of west Greenland during the Greenland Ice margin experiment. J Geophys Res 102(D12):13813–13824

Gallée H, Pettré P (1998) Dynamical constraints on katabatic wind cessation in Adelie Land, Antarctica. J Atmos Sci 55(10):1755–1770

Gallée H, Schayes G (1994) Development of a 3-dimensional meso-gamma primitive equation model—katabatic winds simulation in the area of Terra-Nova Bay, Antarctica. Mon Weather Rev 122(4):671–685

Gallée H, Guyomarc'h G, Brun E (2001) Impact of snow drift on the Antarctic ice sheet surface mass balance: possible sensitivity to snow-surface properties. Boundary-Layer Meteorol 99:1–19

Genthon C, Kaspari S, Mayewski PA (2005) Interannual variability of the surface mass balance of West Antarctica from ITASE cores and ERA40 reanalyses, 1958–2000. Clim Dyn 24(7–8):759–770. doi:10.1007/s00382-005-0019-2

Genthon C, Lardeux P, Krinner G (2007) The surface accumulation and ablation of a coastal blue-ice area near Cap Prudhomme, Terre Adélie, Antarctica. J Glaciol 53(183):635–645. doi:10.3189/002214307784409333

Genthon C, Krinner G, Castebrunet H (2009) Antarctic precipitation and climate change predictions: horizontal resolution and margin vs plateau issues. Ann Glaciol 50:55–60

Grell GL, Dudhia J, Stauffer DR (1994) A description of the fifth-generation Penn State/NCAR mesoscale model (MM5). NCAR technical note NCAR/TN-398CSTR, p 117. National Center for Atmospheric Research, Boulder, Colorado

Helsen MM, van den Broeke MR, van de Wal RSW, van de Berg WJ, van Meijgaard E, Davis CH, Li Y, Goodwin I (2008) Elevation changes in Antarctica mainly determined by accumulation variability. Science 320(5883):1626–1629. doi:10.1126/science.1153894

Hourdin F, Musat I, Bony S et al (2006) The LMDZ4 general circulation model: climate performance and sensitivity to parametrized physics with emphasis on tropical convection. Clim Dyn 27:787–813. doi:10.1007/s00382-006-0158-0

IPCC (2007) Climate change 2007: the physical science basis. Contribution of working group I to the fourth assessment report of the Intergovernmental Panel on Climate Change. Cambridge University Press, Cambridge

King JC, Turner J (1997) Antarctic meteorology and climatology. Cambridge atmospheric and space science series. Cambridge University Press, Cambridge

Kitanidis PK (1997) Introduction to geostatistics: applications to hydrogeology. Cambridge University Press, New York

König-Langlo G, King JC, Pettré P (1998) Climatology of the three coastal Antarctic stations Dumont d'Urville, Neumayer, and Halley. J Geophys Res 103(D9):10935–10946

Krinner G, Genthon C, Li ZX, Le Van P (1997) Studies of the Antarctic climate with a stretched-grid general circulation model. J Geophys Res 102(D12):13731–13745

Krinner G, Magand O, Simmonds I, Genthon C, Dufresne J (2007) Simulated Antarctic precipitation and surface mass balance at the end of the twentieth and twenty-first centuries. Clim Dyn 28(2–3):215–230. doi:10.1007/s00382-006-0177-x

Lenaerts JTM, van den Broeke MR, Déry SJ, König-Langlo G, Ettema J, Munneke PK (2010) Modelling snowdrift sublimation on an Antarctic ice shelf. The Cryosphere 4(2):179–190. doi:10.5194/tc-4-179-2010

Magand O, Genthon C, Fily M, Krinner G, Picard G, Frezzotti M, Ekaykin AA (2007) An up-to-date quality-controlled surface mass balance data set for the 90 degrees-180 degrees E Antarctica sector and 1950–2005 period. J Geophys Res 112(D12):D12106. doi:10.1029/2006JD007691

Magand O, Picard G, Brucker L, Fily M, Genthon C (2008) Snow melting bias in microwave mapping of Antarctic snow accumulation. The Cryosphere 2:109–115

Marti O, Braconnot P, Bellier J et al (2006) The new IPSL climate system model: IPSL-CM4. Note du Pôle de Modélisation n. 26. IPSL, ISSN 1288–1619

Mayewski PA, Meredith MP, Summerhayes CP et al (2009) State of the Antarctic and Southern Ocean climate system. Rev Geophys 47:RG1003. doi:10.1029/2007RG000231

Monaghan AJ, Bromwich DH, Fogt RL et al (2006a) Insignificant change in Antarctic snowfall since the International Geophysical Year. Science 313(5788):827–831. doi:10.1126/science.1128243

Monaghan AJ, Bromwich DH, Wang S (2006b) Recent trends in Antarctic snow accumulation from polar MM5 simulations. Philos Trans R Soc A 364(1844):1683–1708. doi:10.1098/rsta.2006.1795

Pettré P, Pinglot JF, Pourchet M, Reynaud L (1986) Accumulation distribution in Terre Adélie, Antarctica: effect of meteorological parameters. J Glaciol 32(112112):486–500

Richardson-Näslund C (2004) Spatial characteristics of snow accumulation in Dronning Maud Land, Antarctica. Glob Planet Chang 42(1–4):31–43. doi:10.1016/j.gloplacha.2003.11.009

Rignot E, Bamber JL, van den Broeke MR, Davis C, Li Y, van de Berg WJ, van Meijgaard E (2008) Recent Antarctic ice mass loss from radar interferometry and regional climate modelling. Nat Geosci 1(2):106–110. doi:10.1038/ngeo102

Simmons A, Uppala S, Dee D, Kobayashi S (2006) ERA-interim: new ECMWF reanalysis products from 1989 onwards. ECMWF Newslett 110:25–35

Uppala SM, Kallberg PW, Simmons AJ et al (2005) The ERA-40 reanalysis. Q J R Meteorol Soc 131(612):2961–3012. doi:10.1256/qj.04.176

van de Berg WJ, van den Broeke MR, Reijmer C, van Meijgaard E (2006) Reassessment of the Antarctic surface mass balance using calibrated output of a regional atmospheric climate model. J Geophys Res 111:D11104. doi:10.1029/2005JD006495

Vaughan DG, Russell J (1997) Compilation of surface mass balance measurements in Antarctica. Internal rep. ES4/8/1/1997/1. British Antarctic Survey, Cambridge, UK